

## Pairing Symmetry and Flux Quantization in a Tricrystal Superconducting Ring of $\text{YBa}_2\text{Cu}_3\text{O}_{7-\delta}$

C. C. Tsuei, J. R. Kirtley, C. C. Chi,\* Lock See Yu-Jahnes, A. Gupta, T. Shaw, J. Z. Sun, and M. B. Ketchen

IBM Thomas J. Watson Research Center, P.O. Box 218, Yorktown Heights, New York 10598

(Received 21 March 1994; revised manuscript received 19 May 1994)

We have used the concept of flux quantization in superconducting  $\text{YBa}_2\text{Cu}_3\text{O}_{7-\delta}$  rings with 0, 2, and 3 grain-boundary Josephson junctions to test the pairing symmetry in high- $T_c$  superconductors. The magnetic flux threading these rings at 4.2 K is measured by employing a scanning superconducting quantum interference device microscope. Spontaneous magnetization of a half magnetic flux quantum,  $\Phi_0/2 = h/4e$  has been observed in the 3-junction ring, but not in the 2-junction rings. These results are consistent with  $d$ -wave pairing symmetry.

PACS numbers: 74.60.Ge, 74.72.Bk

An unambiguous determination of the order parameter symmetry is crucial to understanding the mechanism responsible for high-temperature superconductivity in the cuprates. For example, a  $d_{x^2-y^2}$  symmetry [ $\Delta(\hat{k}) \sim k_x^2 - k_y^2 \sim \cos 2\theta$ ] in the pairing wave function will lend strong support for pairing mediated by antiferromagnetic spin fluctuations [1]. Theories such as the interlayer coupling model [2] will be supported if  $s$ -wave superconductivity can be demonstrated. On the other hand, the van Hove model [3] is compatible with either symmetry. Recently, there have been numerous experiments [4–6] dealing with various aspects of pairing symmetry in high- $T_c$  superconductors. Unfortunately, the results are ambiguous. The reports in favor of  $d$ -wave pairing are roughly equal in number to those supporting  $s$ -wave symmetry. This unsettling situation partially stems from the often indirect nature of the experimental evidence, as well as experimental issues such as sample quality, impurity scattering, twinning, and trapped magnetic flux. For details, the reader is referred to Ref. [4].

In this Letter an experiment based on flux quantization of a three-grain ring of  $\text{YBa}_2\text{Cu}_3\text{O}_{7-\delta}$  is proposed and applied to test the symmetry of the pair state. The symmetry of a pair wave function can best be probed at the junction interface as the Cooper pairs tunnel across a Josephson junction or weak link [7]. The sign of the Josephson current of a junction between two  $d$ -wave superconductors depends on the relative orientation of their order parameters with respect to the junction interface. As shown recently by Sigrist and Rice [8], the supercurrent  $I_s^{ij}$  can be expressed by

$$I_s^{ij} = (A^{ij} \cos 2\theta_i \cos 2\theta_j) \sin \Delta \phi_{ij} = I_c^{ij} \sin \Delta \phi_{ij}, \quad (1)$$

where  $A^{ij}$  is a constant characteristic of junction  $ij$ , and  $\theta_i$  and  $\theta_j$  are angles of the crystallographic axes (or equivalently wave vectors  $k_x$  and  $k_y$ ) with respect to a junction interface (e.g., a grain boundary) between superconductors  $i$  and  $j$ .

In the case of  $s$ -wave symmetry, the sign of  $I_s^{ij}$  is a constant of  $\theta_i, \theta_j$ , but its magnitude can vary due to gap anisotropy. For the case of a single superconduct-

ing ring with one Josephson junction, Sigrist and Rice showed that, based on free energy considerations, the ground state of a ring with one  $\pi$  junction (i.e.,  $I_c^{ij} < 0$ ) has a spontaneous magnetization if the critical current is sufficiently large. The magnetic flux threading through such a  $\pi$  ring is exactly half of the flux quantum ( $\Phi_0/2 = h/4e = 1.035 \times 10^{-7} \text{ G cm}^2$ ) when the external field  $H_{\text{ext}} = 0$  and the condition  $L|I_c| > \Phi_0$ , where  $L$  is the self-inductance of the ring, is satisfied. In the case of a multiple-junction ring, Sigrist and Rice [8] suggested that a ring of odd-number  $\pi$  junctions will also exhibit  $\Phi_0/2$  spontaneous magnetization. In the following, we show that this is indeed true. In reference to the odd-number  $\pi$ -junction ring in Fig. 1 and Eq. (1), the flux quantization of a superconducting ring can be written as follows:

$$\Phi_{\text{ext}} + I_s L + \frac{\Phi_0}{2\pi} \sum_{ij} \Delta \phi_{ij} = n \Phi_0, \quad (2)$$

where  $I_s$ , the current circulating in the ring, is given by

$$I_s = I_c^{12} \sin \Delta \phi_{12} = I_c^{23} \sin \Delta \phi_{23} = I_c^{ij} \sin \Delta \phi_{ij}. \quad (3)$$

Equations (2) and (3) are valid for both  $s$ -wave and  $d$ -wave rings. In the case of a ring with an odd number of  $\pi$  junctions, it is sufficient to consider the case where only one critical current is negative (say  $I_c^{12} = -|I_c^{12}|$ ). Then  $I_s = |I_c^{12}| \sin(-\pi + \Delta \phi_{12})$ . For zero external field,  $\Phi_{\text{ext}} = 0$ ,  $n = 0$ , and  $|I_c^{12}|L \gg \Phi_0$ ,  $I_c^{ij}L \gg \Phi_0$ , the flux quantization condition Eq. (2) will lead to the following expression for the circulating current:

$$I_s = \frac{\pi}{2\pi(L/\Phi_0) + 1/|I_c^{12}| + 1/I_c^{23} + \dots} \approx \frac{\Phi_0}{2L}. \quad (4)$$

Equation (4) is essentially a restatement of the spontaneous magnetization of an odd-number  $\pi$ -junction ring.

It should be pointed out that the Sigrist-Rice formula, Eq. (1), is based on an implicit assumption that the junction interface is perfectly smooth and without any disorder. In reality, the electron wave vector orthogonal to the junction face can be significantly distorted by interface roughness, impurities, strain, oxygen deficiency, etc.

To model the disorder effect, one can consider the consequence of an angular deviation  $\Delta\theta$  from the perfect junction interface. The results of a straightforward calculation can be expressed as

$$I_s = \frac{1}{2} A^{ij} \{ \cos 2(\theta_i + \theta_j) + B^{ij}(\alpha) \cos 2(\theta_i - \theta_j) \} \sin \Delta \phi_{ij}, \quad (5)$$

where  $B^{ij}(\alpha)$  is a function of the angular distribution probability  $P(\theta)$  of  $\theta_i$  and  $\theta_j$ ,  $\int_{-\alpha}^{\alpha} P(\theta) d\theta = 1$ , and  $\alpha$  is a measure of the angular variation of  $\theta$ . As a consequence of the fourfold symmetry in the Cu-O square lattice in the  $\text{CuO}_2$  planes, the maximum disorder at the grain boundary corresponds to  $\alpha = \pi/4$ . This leads to  $B^{ij}(\pi/4) = 0$ , and a maximum-disorder formula for the circulating current:

$$I_s^{ij} = I_c^{ij} \cos 2(\theta_i + \theta_j) \sin \Delta \phi_{ij}. \quad (6)$$

Given Eq. (1) and Eq. (6), one can design a  $d$ -wave pairing symmetry test for cuprate superconductors that is valid for all cases. The basic idea of our experiment is to fabricate a trigrain boundary-junction ring of high- $T_c$  superconductor such as  $\text{YBa}_2\text{Cu}_3\text{O}_{7-\delta}$ . A scanning SQUID (superconducting quantum interference device) [9] microscope is then used to image the magnetic flux threading through the superconducting trigrain ring to search for the  $\Phi_0/2$  spontaneous magnetization.

The three-junction rings used in this work are fabricated from epitaxial films of  $\text{YBa}_2\text{Cu}_3\text{O}_{7-\delta}$  deposited on a (100) tricrystal  $\text{SrTiO}_3$  substrate [10] (Fig. 1) by using standard pulsed laser deposition. The  $\text{YBa}_2\text{Cu}_3\text{O}_{7-\delta}$  film is  $c$ -axis oriented with  $c = 11.685 \text{ \AA}$  and a zero-resistance transition temperature of 90.7 K. The misorientation across each grain boundary in the tricrystal substrate (as indicated in Fig. 1) was determined from backscattered Kikuchi maps recorded from each crystal using the electron beam probe of a scanning electron microscope. For each boundary the misorientation angle was within  $4^\circ$  of the design misorientation angle of  $30^\circ$ . The rotation axes of the boundaries was close to the normal to the plane of the sample, showing that the boundaries are primarily of tilt type character.

In this experiment, four rings (inner diameter  $48 \mu\text{m}$ , width  $10 \mu\text{m}$ ) are patterned using a standard photolithographic process. To test the quality of the individual grain boundary junctions across each grain boundary, bridges  $25 \mu\text{m}$  in length and  $10 \mu\text{m}$  in width across each grain boundary are prepared on bicrystal substrates that were cut off from the tricrystal substrate. The epitaxial  $\text{YBa}_2\text{Cu}_3\text{O}_{7-\delta}$  films for these junctions were laser deposited in the same run and in close proximity to the tricrystal substrate for the four rings. The values of  $I_c^{ij}$  ( $J_c^{ij}$ ) for these three test junctions agree within 20%.  $I_c^{12}$  ( $J_c^{12}$ ), for example, is found to be 1.8 mA ( $1.5 \times 10^5 \text{ A/cm}^2$ ). The resistance as a function of temperature,  $R(T)$ , for the bridge across a grain boundary has a small shoulder below the

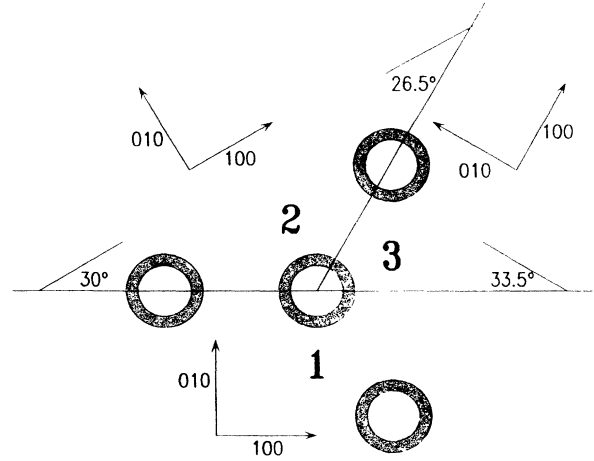


FIG. 1. Schematic diagram for the tricrystal (100)  $\text{SrTiO}_3$  substrate, with four epitaxial  $\text{YBa}_2\text{Cu}_3\text{O}_{7-\delta}$  rings.

$T_c$  ( $= 90.7 \text{ K}$ ) characteristic of a grain boundary weak link. The  $IV$  curve ( $T = 4.2 \text{ K}$ ) exhibits a typical resistively shunted Josephson junction characteristic. From the  $I_c^{ij}$  value and the estimated self-inductance of rings ( $L \approx 100 \text{ pH}$ ) one finds that the  $LI_c^{ij}$  product is about  $100\Phi_0$ , easily satisfying the condition  $LI_c^{ij} \gg \Phi_0$  of Eq. (4). Therefore, a spontaneous magnetization of  $\Phi_0/2$  at  $\Phi_{\text{ext}} \sim 0$  should be observable in our 3-junction ring.

Figure 2 shows a scanning SQUID microscope [9] image of the four rings in our experiment. This image was obtained by scanning the pickup loop of a SQUID [shown schematically in Fig. 3(a)] relative to the sample at 4.2 K. The loop center was  $10 \mu\text{m}$  from the sharpened tip of its substrate, which was in direct contact with the sample, and rotated approximately  $20^\circ$  away from the sample plane, with the leads oriented towards the top of the image. The sample was mounted on a flexible cantilever, so that the tip remained in contact while scanning. The SQUID was operated in flux-locked mode, with noise approximately  $2 \times 10^{-6} \Phi_0/\text{Hz}^{1/2}$ . The ratio of the mutual inductance between loop and ring to the self-inductance of the ring is about 0.02, so that the effect of the SQUID flux coupling back into the ring should be small. Our interpretation of this image (run 12 in Fig. 3) is that the upper-right and left 2-junction rings, and the lower-right 0-junction ring, have no flux threading them, while the center 3-junction ring has  $1/2$  of the flux quantum  $h/2e$  threading it. The outer control rings are visible through mutual inductance coupling between the rings and the SQUID loop. We determine the amount of flux in the central ring as follows.

The mutual inductance  $M(\rho)$  between a pickup loop tilted at an angle  $\theta$  from the sample ( $x$ - $y$ ) plane in the  $x$ - $z$  plane, and a circular wire of radius  $R$  at the origin, is given by

$$M(\rho) = \frac{\mu_0 R}{4\pi} \int d^2x \int_0^{2\pi} d\phi \frac{\cos\theta(R - y \sin\phi - x \cos\phi) - \sin\theta(z \cos\phi)}{(x^2 + y^2 + z^2 + R^2 - 2xR \cos\phi - 2yR \sin\phi)^{3/2}}, \quad (7)$$

where the integral  $d^2x$  is over the plane of the pickup loop, and the vector  $\rho$  specifies the displacement of the pickup loop with respect to the ring in the  $x$ - $y$  plane. We calculate  $M(0) = 2.4$  pH for the as fabricated tip centered above a  $29 \mu\text{m}$  radius ring, at a tilt angle of  $20^\circ$ . A given flux  $\Phi$  threading a superconducting ring with self-inductance  $L$  induces a circulating current  $I_r = \Phi/L$  around the ring, which in turn induces a flux  $\Phi_s(\rho) = M(\rho)\Phi/L$  in the pickup (sensor) loop. We calculate the inductance of our rings to be  $99 \pm 5$  pH.

The solid lines in the bottom part of Fig. 2 are model calculations for the cross sections indicated by the contrasting lines in the image, assuming  $\Phi = \Phi_0/2 = h/4e$  in the 3-junction ring. The asymmetry in the images results from the tilt of the pickup loop, as well as the asymmetric pickup area from the unshielded section of the leads. Using  $\Phi_0/2$  for the flux in the 3-junction ring results in much better agreement than would be obtained using  $\Phi_0$ .

Our value for  $M(0)$  was checked by positioning the pickup loop in the centers of the rings and measuring the SQUID output vs field characteristic. Representative results for the 3-junction ring are shown in Fig. 3(a). In this figure a linear background, measured by placing the

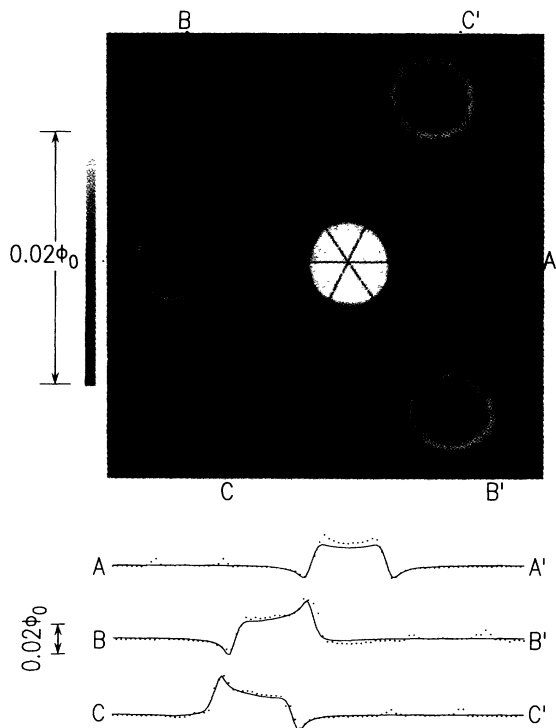


FIG. 2. Scanning SQUID microscope image of the four superconducting rings in Fig. 1, cooled in a field  $<5$  mG. The dots are cross sections through the data as indicated by the contrasting lines. The solid lines are calculations assuming the 3-junction ring has  $\Phi_0/2$  flux threading it.

loop over the center of the 0-junction control ring, has been subtracted out. The upper inset in this figure shows the sensor flux vs field characteristic over a larger field range. At low fields stepwise admission of flux into the ring leads to a staircase pattern, with progressively smaller heights and widths to the steps, until over a small intermediate field range, single flux quanta are admitted. In the main part of Fig. 3(a), single flux quanta are admitted. At larger fields the steps disappear and the SQUID flux vs field characteristic slowly oscillates about a mean line. The heights of the single flux-quantum steps in the intermediate field region, derived by fitting the data with a linear staircase (dashed line) are  $\Delta\Phi_s = 0.0237\Phi_0$ . This is in good agreement with our calculated value of  $\Delta\Phi_s = M(0)\Phi_0/L = (0.024 \pm 0.003)\Phi_0$ . Twelve repetitions of this measurement, including measurements of both the 2-junction and 3-junction rings, gave values of  $M(0)\Phi_0/L =$

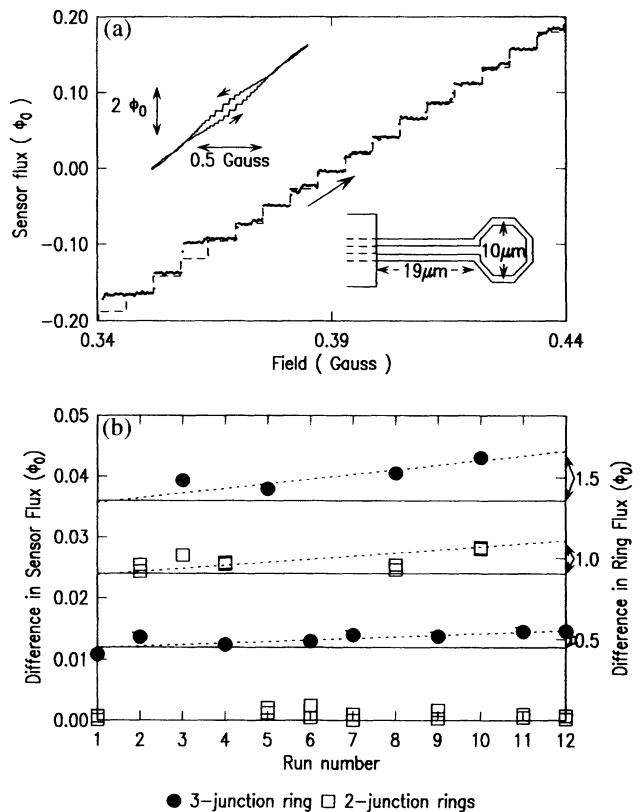


FIG. 3. (a) The measured SQUID flux vs field characteristic with the SQUID pickup coil centered on the 3-junction ring. The upper left inset shows the flux-field characteristic over a larger field range. The lower right inset shows the geometry of the SQUID pickup loop, with  $1.2 \mu\text{m}$  linewidths and spacings. (b) The result of 12 separate cooldowns of the sample in nominal zero field. The solid lines are our calculations for the as-fabricated tip, the dashed lines include a correction for tip wear.

$(0.028 \pm 0.005) \Phi_0$ . The large uncertainties in these calibration runs have two sources: Small misalignments in the position of the loop relative to the center of the rings result in relatively large errors, as can be seen from the cross sections of Fig. 2. Further, the step heights on average increase with time, as the tip wore while taking  $\approx 100$  images in direct contact with the sample, moving the pickup loop progressively closer to the ring plane. Visual inspection of the loop at the end of these measurements showed extensive wear, such that the point of contact was within  $2 \mu\text{m}$  of the pickup loop edge.

We calibrated our fields by replacing the sample with a large pickup area SQUID magnetometer. Our measured fields agree with our calculations to within about 3%. The widths of the steps, averaging over 11 measurements for increasing positive fields, was  $5.7 \pm 1$  mG. This is about 25% smaller than  $\Delta B = \Phi_0/A_{\text{ring}}$ , where  $A_{\text{ring}} = 2715 \mu\text{m}^2$  is the effective area of the rings. This is not too surprising, given the nonequilibrium nature of the flux penetration process, as indicated by the hysteresis in the flux-field characteristic. The average slope of the flux-field characteristic does, however, agree within experimental error with the effective area of the rings.

Figure 3(b) summarizes the results from 12 cooldowns of the sample. We plot the absolute value of the difference between the SQUID loop flux in the centers of the 2-junction or 3-junction rings, and the 0-junction control ring. Since each point was taken from a full image, we could judge the center of the rings with accuracy, and our data scatter is much smaller than in the calibration runs. The solid lines are the expected values for the flux difference, calculated as described above. In all of our measurements  $\Delta\Phi$  always fell close to  $(N + 1/2)h/2e$  for the 3-junction ring, and close to  $Nh/2e$  for the 2-junction rings ( $N$  an integer). However, there is clearly some drift to the data, which we associate with tip wear. A fit to the eight  $\Phi_0/2$  points in Fig. 3(b), assuming exactly  $h/4e$  flux threads the 3-junction rings, implies that the mutual inductance  $M(0) = 2.4$  pH for the as fabricated tip, and increases to 2.9 pH at the end of the series. For comparison, our calculations give 2.4 pH for the center of the loop  $10 \mu\text{m}$  from the tip end, and 2.7 pH for the tip end just at the edge of the pickup loop. The dashed lines, including this correction to the mutual inductance, agree remarkably well with the data.

One can infer the inductance of the rings from the high-field asymptotic difference between the flux in a ring with junctions and the flux in the ring without junctions (Fig. 3). At the end of our measurement series this (SQUID) flux was  $(4.0 \pm 0.2)\Phi_0/G$  of applied field. Using  $L = A_{\text{ring}}M(0)/(d\Phi_s/dB)$ , and a mutual inductance of 2.9 pH, gives  $L = 95 \pm 5$  pH, in good agreement with our calculation of  $L = 99 \pm 5$  pH. For our present interpretation to be incorrect, (1) our calculations of the inductances would have to be incorrect by a factor of 2, (2) the flux steps in our calibration runs would have to go immediately from 2 flux quanta/step to no steps, and (3) the flux in the

3-junction ring would have to always be odd-integer values different from the control ring, while the 2-junction rings would always have to have even integer differences from the control. This seems extremely unlikely.

Although our results are consistent with  $d$ -wave pairing symmetry, this experiment alone cannot rule out even parity states with an order parameter symmetry varying as  $\Delta \sim \cos(4\theta)$  [11]. It has also been proposed that magnetic spin-flip scattering or correlation effects at the grain boundary can induce a  $\pi$  shift in the superconducting order parameter phase at each grain boundary [12].

In summary, we have directly observed for the first time spontaneous magnetization of  $\pm\Phi_0/2$  in a 3-junction ring of epitaxial  $\text{YBa}_2\text{Cu}_3\text{O}_{7-\delta}$ . This observation supports  $d$ -wave pairing symmetry.

The scanning SQUID microscope used for this work was developed under the auspices of the Consortium for Superconducting Electronics. The authors wish to thank D.H. Lee for many stimulating discussions, in particular on the effect of disorder on the grain-boundary characteristics. They are thankful to W. Gallagher, D.M. Newns, P. Chaudhari, and other colleagues for useful discussions. The technical assistance of G. Trafas, M. Cali, and J. Hurd is greatly appreciated.

---

\*Present address: Materials Science Center and Department of Physics, National Tsing-Hua University, Taiwan, Republic of China.

- [1] For example, N.E. Bickers, D.J. Scalapino, and S.R. White, *Phys. Rev. Lett.* **62**, 961 (1989); P. Monthoux, A.V. Balatsky, and D. Pines, *Phys. Rev. B* **46**, 14 803 (1992).
- [2] S. Chakravarty *et al.*, *Science* **251**, 337 (1993).
- [3] R.S. Markiewicz, *J. Phys. Condens. Matter* **2**, 665 (1990); D.M. Newns *et al.*, *Comments Condens. Matter Phys.* **15**, 273 (1992); C.C. Tsuei *et al.*, *Phys. Rev. Lett.* **69**, 2134 (1992), and references therein.
- [4] For a brief review, see an article by B.G. Levi, in *Phys. Today* **46**, No. 5, 17 (1993), and references therein; also the letters in *Phys. Today* **47**, No. 2, 11 (1994).
- [5] D.A. Wollman *et al.*, *Phys. Rev. Lett.* **71**, 2134 (1993).
- [6] P. Chaudhari and Shawn-Yu Lin, *Phys. Rev. Lett.* **72**, 1084 (1994).
- [7] V.B. Geshkenbein, A.I. Larkin, and A. Barone, *Phys. Rev. B* **36**, 235 (1987).
- [8] Manfred Sigrist and T.M. Rice, *J. Phys. Soc. Jpn.* **61**, 4283 (1992).
- [9] F.P. Rogers, BS/MS thesis, EICS Department, MIT (1983); R.C. Black *et al.*, *Appl. Phys. Lett.* **62**, 2128 (1993); L.N. Vu, M.S. Wistrom, and D.J. van Harlingen, *Appl. Phys. Lett.* **63**, 1693 (1993).
- [10] Tricrystal designed by the authors and manufactured by Shinkosa Co., Tokyo.
- [11] C.M. Varma (private communication).
- [12] L.N. Bulaeviski, V.V. Kuzii, and A.A. Sobyenin, *JETP Lett.* **25**, 290 (1977); B.I. Spivak and S. Kivelson, *Phys. Rev. B* **43**, 3740 (1991).

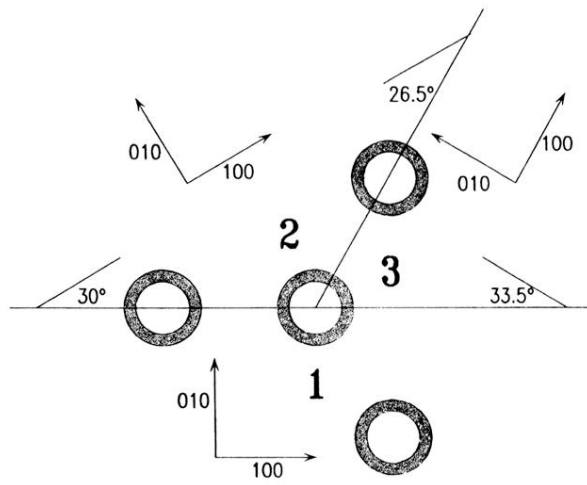


FIG. 1. Schematic diagram for the tricrystal (100)  $\text{SrTiO}_3$  substrate, with four epitaxial  $\text{YBa}_2\text{Cu}_3\text{O}_{7-\delta}$  rings.

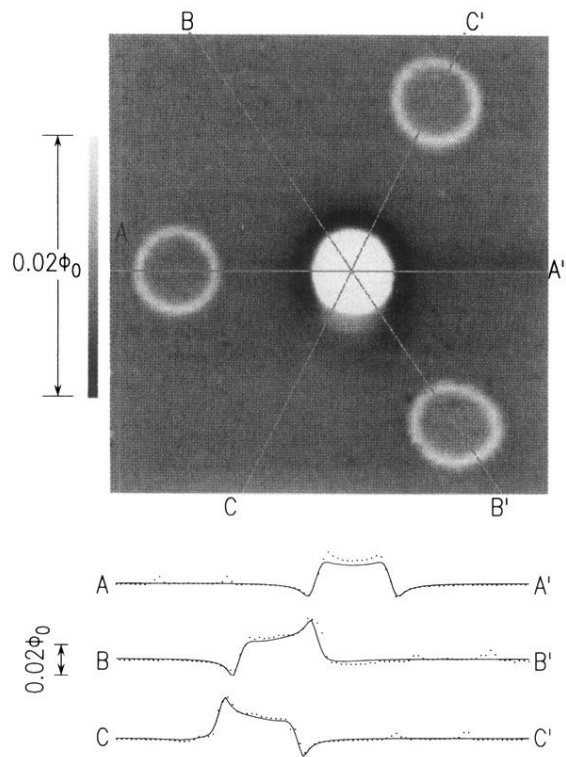


FIG. 2. Scanning SQUID microscope image of the four superconducting rings in Fig. 1, cooled in a field  $<5$  mG. The dots are cross sections through the data as indicated by the contrasting lines. The solid lines are calculations assuming the 3-junction ring has  $\Phi_0/2$  flux threading it.